

## THE ELECTRODYNAMICS AND MAGNETOHYDRODYNAMICS OF GEOSPACE

M. J. RYCROFT

*British Antarctic Survey, NERC, Madingley Road, Cambridge CB3 0ET, U. K.*

**Abstract:** The rationale for undertaking research on geospace is first reviewed. Overlooking time-dependent aspects of the problem, attention is concentrated on the steady state, magnetohydrodynamic interaction of the solar wind with the magnetosphere, and on the macroscopic treatment of ionospheric convection over the polar cap. The law of the conservation of magnetic flux out of the southern polar cap into the interplanetary medium is applied, as it is for the flux into the northern polar cap from interplanetary space above the ecliptic plane. Some recent radar results are mentioned, and some suggestions made for further experimental research, both in space and from the ground in the polar regions.

### 1. Introduction

This paper is composed of three parts. The first, a preamble, gives a personal rationale for carrying out research on geospace, on ionospheric and magnetospheric physics in the polar regions, in the 1980s and 90s. Whereas the late 1950s and 1960s were periods of discovery and exploration, attention turned in the 1970s towards understanding and explaining the phenomena observed. For the future, the prediction of conditions in the geospace environment will be the emphasis.

In this field, international research programmes provide the necessary impetus. After the International Magnetospheric Study (IMS), carried out from 1976-1979, the all-embracing programme for the 1990s will be the Solar Terrestrial Energy Program (STEP). Its aim is to investigate the mass, momentum and energy transfer chain from the Sun to the Earth's upper atmosphere, through the geospace plasma environment. Emphasis will be placed here on the physics of energy transformations, conversions of energy from one form to another. For a steady solar wind, magnetohydrodynamics (MHD) is often, but not always, a good approximation. However, many electrodynamic properties of a plasma rely on phenomena such as wave-particle interactions, where the approximations of MHD break down.

In such international programmes, it will be essential to have ground-based experiments complemented by experiments carried out on balloons, rockets and satellites. Further, it will be essential to devote sufficient resources to data processing and analysis, especially collaborative analysis between different groups who have different data sets, and particularly using computers; to aid interpretation, it will be essential to have strong programmes of fundamental theoretical research and computer modelling.

The second part of the paper is concerned with a discussion of the magnetic flux emanating from the Antarctic polar cap and entering the interplanetary medium. It

is concerned also with the same amount of magnetic flux entering the northern lobe of the magnetospheric tail and entering the northern polar cap. The idea for this treatment came during a re-read of the brief paper by DUNGEY (1965) which contains the seminal idea that a geomagnetic field line is connected to the interplanetary magnetic field (IMF). For simplicity, the IMF is treated as being southward. An interplanetary magnetic flux tube connected to a magnetospheric flux tube is pulled across the polar cap, from the noon auroral oval (or cusp region) to the midnight auroral oval, as the flux tube is dragged down the tail of the magnetosphere by the solar wind. The length of the tail is determined by this physical process.

The third and final part of the paper is concerned not only with recent results in this field of endeavour, but also with present and future research programmes designed to answer the remaining important physical questions on the Earth's plasma environment.

## 2. Background Rationale for Geospace Research

AKASOFU (1980) states that "the interaction between a magnetised celestial body and a magnetised plasma flow with a varying magnetic field is a seemingly simple problem that discloses a number of fundamental plasma processes in cosmic electrodynamics. The magnetosphere provides a perfect "laboratory" for investigating those plasma processes." The plasma physics learnt thereby may be applied elsewhere in the Universe, for example in astrophysical plasmas and in laboratory fusion devices. The Earth's ionosphere and magnetosphere not only form an ideal laboratory for such research but also the only laboratory that is accessible to Man where detailed, *in situ* experiments on a cosmic plasma can be conducted. The plasma contained in the magnetosphere has two sources, namely the solar wind and the ionosphere.

AKASOFU (1980) also hints that the problem is a time dependent one; hence, it is a difficult problem. It is easier to consider, first, the steady-state problem, an average state of affairs, an average of the time dependent phenomena that are actually occurring. The importance of the time dependence of magnetospheric and ionospheric processes is becoming increasingly realised. The spectrum of the temporal fluctuations is wide, with periods ranging from 2.2 decades, characteristic of a full solar cycle, to tenths of microseconds for some wave phenomena. This covers sixteen orders of magnitude! Spatial variations also need to be considered. Spatial variations occur on a scale from several Earth radii down to the Debye length, one millimetre in the ionospheric plasma. This range is eleven orders of magnitude. Spatial variations in the solar wind, moving at several hundred kilometres per second past the magnetosphere are equivalent to time variations. Boundaries between different types of plasma can be very narrow; also, inhomogeneities and irregularities in the plasma contribute important effects.

ALFVÉN (1981) considers that "plasma phenomena should be described not only by magnetic field models but also by explicitly accounting for electric currents and the electric circuits in which these flow." Magnetic field lines have no physical reality—they are a figment of Faraday's imagination. In geospace, curl  $B$  usually depends just on  $J$ , the current density. Currents flowing along field lines parallel to the mag-

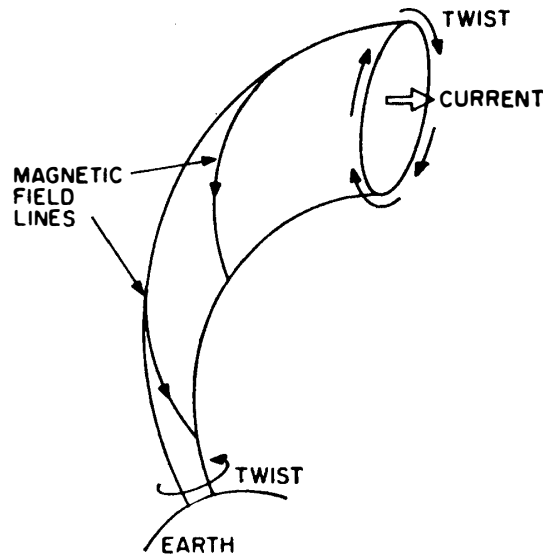


Fig. 1. Diagram illustrating that field aligned currents twist a geomagnetic flux tube.

netic field are associated with field line twisting. This is indicated in Fig. 1. Downcoming auroral electrons, of perhaps a few keV, and upward moving ions link the auroral ionosphere with the outer regions of the magnetosphere. The direction of the upward field aligned electric current departs from the geomagnetic field direction by a fraction of a degree in regions where these large field aligned currents flow in the topside ionosphere. There is a twist of a few tens of degrees associated with the so-called flux transfer event at the magnetopause; this may be caused by a change in the direction of the IMF or by the arrival of an interplanetary sector boundary in the Earth's vicinity.

Electric currents flow horizontally in the ionosphere, as the auroral electrojet, and complete the electric circuit to the outer magnetosphere via upward moving thermal or suprathermal electrons or downward moving ions on flux tubes that are adjacent to the primary auroral flux tubes themselves. Electric currents can also flow in field aligned sheets, aligned in magnetic longitude or in  $L$  shell (McILWAIN, 1961). Instead of causing, as line currents do, a twist in the magnetic field, these sheet currents cause a shear in the magnetic field; the sheet currents transmit stress from one part of the magnetosphere to another.

A crucial problem in geospace plasma physics is the interaction of the solar wind with the Earth's magnetosphere. SONNERUP (1985) has treated the problem magneto-hydrodynamically. This treatment is valid only when the assumptions inherent in MHD are valid. In the magnetospheric boundary layer where the magnetic field is  $B_{BL}$  and the velocity is  $v_{BL}$ , the "electric field  $E_{BL} = -v_{BL} \wedge B_{BL}$  is produced by the tailward motion of the plasma in the layer. If this electric field is projected into the ionosphere, assuming equipotential magnetic field lines, a ionospheric electric field  $E_i$  results. This electric field drives an ionospheric Pedersen current,  $J_i$ , which is fed by a Birkeland current,  $J_{\parallel}$ , at the inner edge of the boundary layer. This current in turn is fed by a cross-field current distribution  $J_{BL}$  in the equatorial boundary layer. The result is that the low latitude boundary layer acts as an electrical generator,  $E_{BL} \cdot$

$J_{BL} < 0$ , and the ionosphere as a load,  $E_1 \cdot J_1 > 0$ . It is also clear that the  $J_1 \wedge B_1$  force acts to produce convective motion of the ionospheric plasma whereas the  $J_{BL} \wedge B_{BL}$  force acts to slow down the boundary layer flow.” The concept of a solar wind/magnetosphere dynamo, acting as an electrical generator, and of the ionosphere acting as a “drag” on the magnetosphere, a load, is a useful one. The dynamo can initially accelerate the ionosphere, which then can act as a flywheel. If the EMF of the solar wind/magnetosphere dynamo decreases enough, the ionosphere changes its role to that of a generator, and causes magnetospheric plasma to move. This simple example of

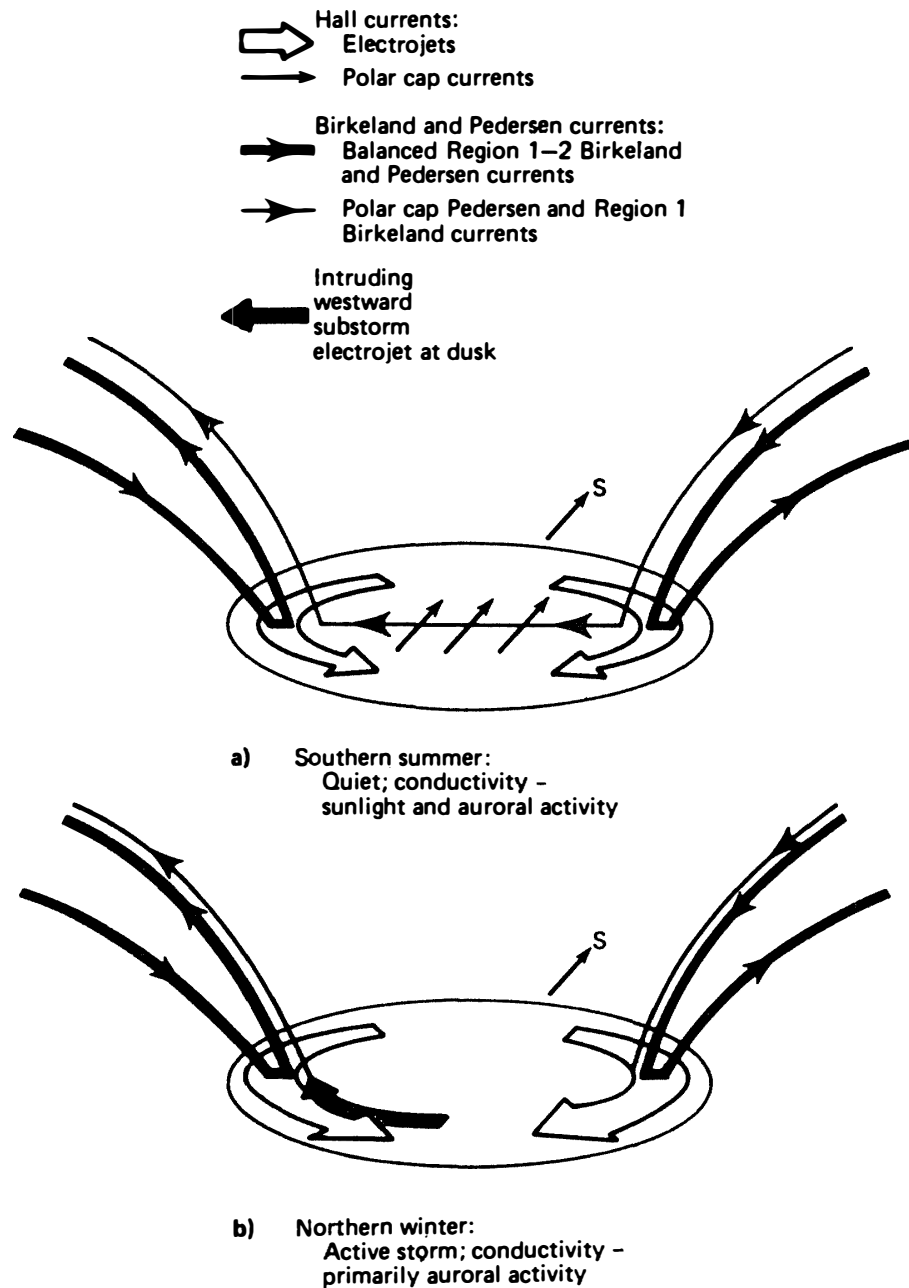


Fig. 2. Diagram illustrating how field aligned currents close in the auroral and polar cap ionosphere, (a) for southern summer, quiet conditions, and (b) for northern winter, active conditions.

a time dependent situation clearly illustrates the interactive coupling between magnetosphere and ionosphere, down and up geomagnetic field lines.

Electric currents cause perturbations to the geomagnetic field, according to the Biot-Savart Law. Observations of geomagnetic disturbances on the ground and aboard spacecraft can be interpreted to give information on the electric currents which flow. The electric circuits flowing in the polar regions are depicted schematically in Fig. 2, a) for summer conditions and b) for winter conditions. The different magnitude of the ionospheric conductivity, determined by the plasma concentration, explains the markedly different patterns. The summer-time pattern is consistent with the well known twin vortex convection, in a horizontal plane, of the ionospheric plasma within the auroral oval, that is in the polar cap. Such flow patterns also exhibit shear, strong gradients of velocity and even reversals of velocity. Collisions between the ions and neutrals cause the ionosphere to pull the thermosphere along. Magnetospheric processes also cause heating of the neutral thermosphere, both by Joule dissipation and by the production of additional ionisation.

The most important time dependent phenomenon in macroscopic magnetospheric physics is the magnetospheric substorm. MCPHERRON (1979) defines the magnetospheric substorm as "a transient process initiated on the nightside of the Earth in which a significant amount of energy derived from the solar wind/magnetosphere interaction is deposited in the auroral ionosphere and magnetosphere." The initial phase of a substorm lasts only one or two minutes, the time that it takes for an Alfvén wave to propagate from the magnetotail down to the auroral ionosphere; the aurora near local midnight brightens considerably then. The substorm itself typically lasts some tens of minutes, or approaching an hour. ATKINSON (1984) has proposed a feedback system coupling the ionosphere and magnetosphere in an unstable mode in order to explain the auroral substorm. This involves the diversion of the cross-tail current into field aligned currents which flow into the ionosphere, and the depletion of plasma in the outer magnetosphere by these field aligned currents. This is shown schematically in Fig. 3.

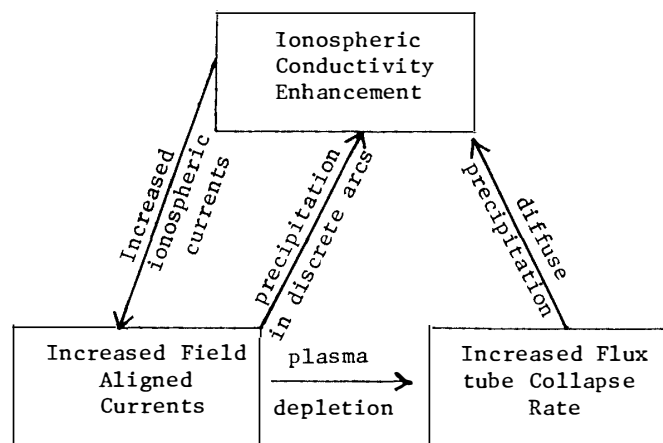


Fig. 3. Mechanistic diagram, showing feedback links, to explain an auroral substorm, from ATKINSON (1984).

### 3. Conservation of Magnetic Flux Applied to the Geospace Environment

COWLEY (1980) has depicted the noon midnight meridian of the magnetosphere, under the influence of a purely southward interplanetary magnetic field (IMF), as shown in Fig. 4. The solar wind moving away from the Sun around the magnetosphere, carrying a southward magnetic field, produces an electric field directed everywhere from dawn to dusk. The magnitude of this electric field  $E$  is, in the MHD approximation, given by  $-v\Delta B$ . The direction of the flow of plasma through the magnetosphere in this MHD treatment, at a velocity  $v=E\Delta B/B^2$ , is shown as the short-dash lines in Fig. 4. Regions where  $E\cdot J$  is greater than zero, or where  $J\cdot E$  is greater than 0, are shown as circled dots. These correspond to regions where the plasma gains energy from the fields. Conversely, regions where  $E\cdot J$  is less than zero (where  $J\cdot E$  is less than 0), shown as circled crosses, illustrate where plasma loses energy to electric and magnetic fields. The aurora occurs on field lines which are catapulted towards the Earth from the reconnection line in the centre of the magnetospheric tail.

Figure 5a, taken from COWLEY (1984), shows the coordinate system used, in a three dimensional diagram. Flow in the equatorial plane is illustrated in Fig. 5b,

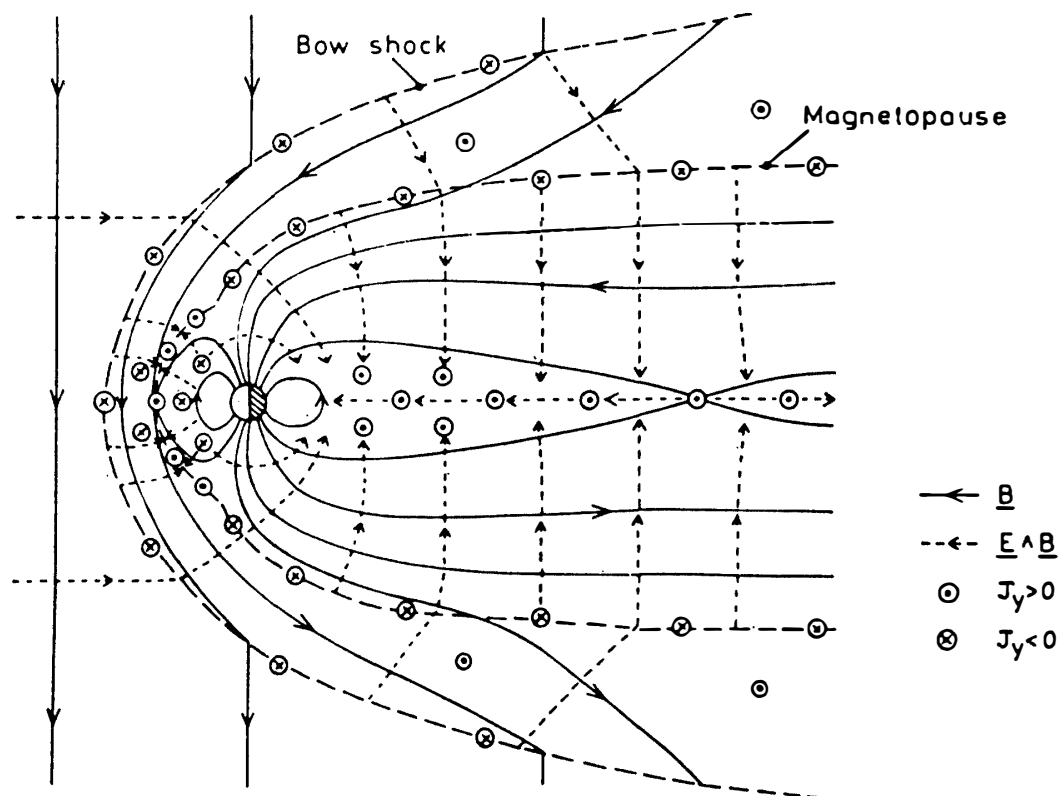


Fig. 4. The reconnection model of the magnetosphere (after COWLEY, 1980) for a southward interplanetary magnetic field. The magnetic field lines are shown solid. The electric field is everywhere from dawn to dusk, and the direction of  $E \wedge B$  is shown by the short-dash lines. The circled dots and crosses indicate the directions of current flow in current layers (dashed lines). Regions where  $E \cdot J > 0$  (dots) and  $E \cdot J < 0$  (crosses) show where the plasma gains or loses energy, respectively.

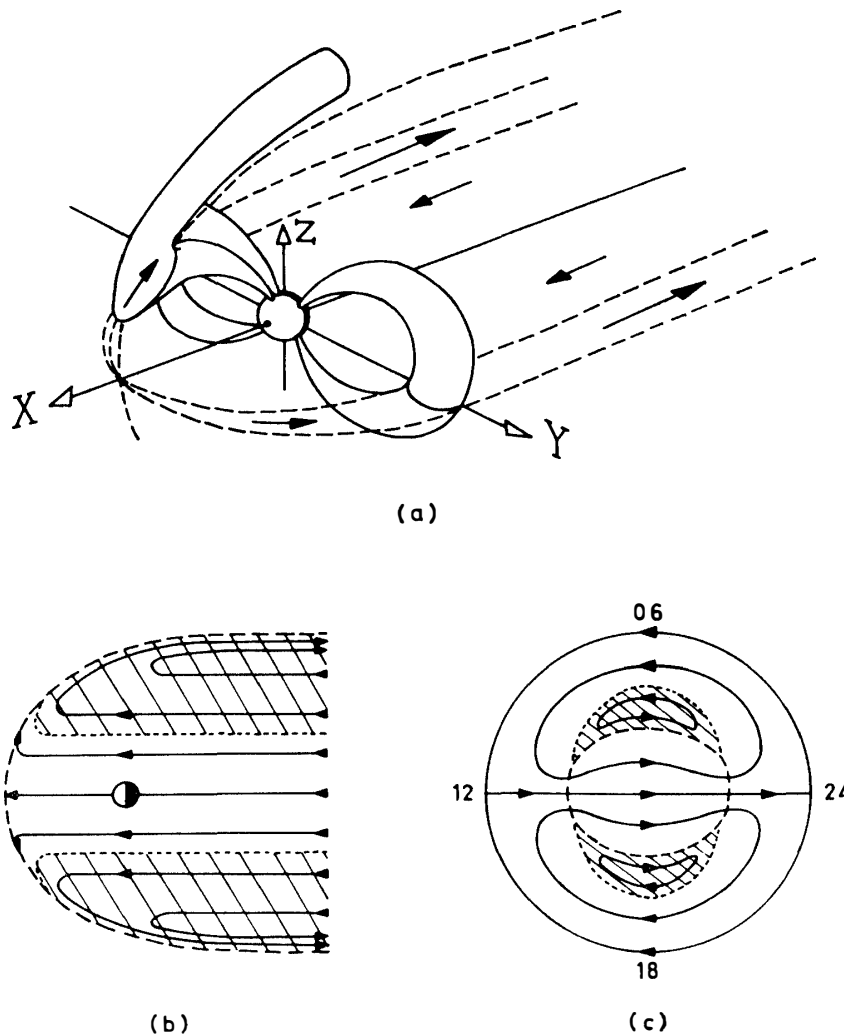


Fig. 5. (a) Diagram illustrating a flux tube convecting across the polar cap, and a dawn and also a dusk flux tube pulled along the flanks of the magnetospheric tail.  
 (b) Plasma flow lines shown in the equatorial plane.  
 (c) Plasma flow lines mapped into the high latitude ionosphere, the numbers showing local time.

and clearly shows the flow of plasma from the tail towards the Earth on the nightside, and out towards the magnetopause on the dayside. In a boundary layer region shown shaded, the flow reverses on the outer flanks of the magnetosphere, the solar wind pulling flux tubes down the tail. In Fig. 5c, this flow pattern is projected down flux tubes to the northern high latitude ionosphere. The polar cap is the almost circular region bounded by dashes, with plasma convecting from the dayside to the nightside, and the return flows taking place at lower latitudes; two convection cells, a dawn one and a dusk one are formed. Figure 6 illustrates the essence of the physics of the situation. Magnetic flux tubes connected to the northern polar cap ionosphere are convected at velocity  $v_{pe1}$  from the dayside to the nightside across the northern polar cap. Magnetic flux entering the polar cap has arrived through the tail of the magnetosphere, the region shown hatched on the right. The total length of the tail,  $l_t R_E$ , is then defined

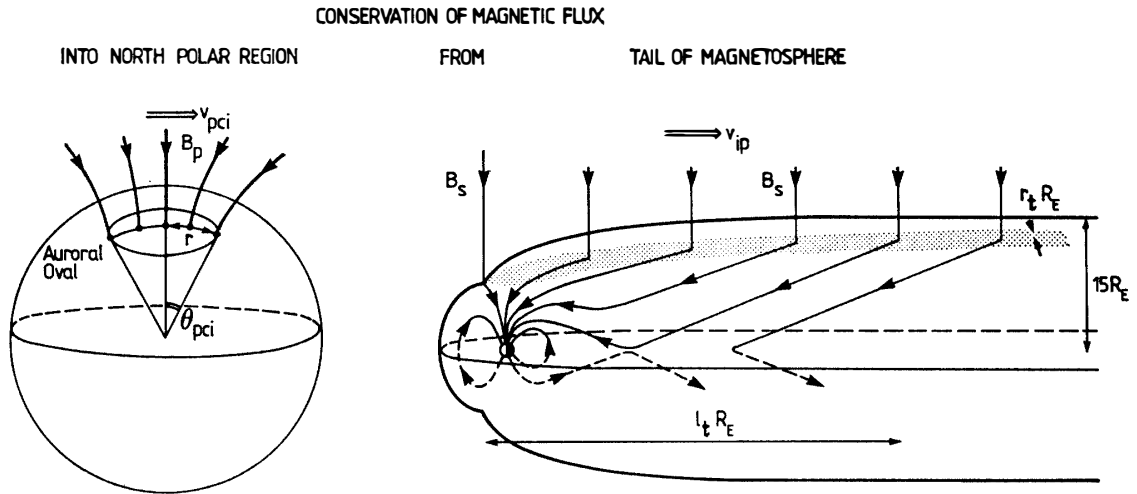


Fig. 6. Diagram illustrating the conservation of magnetic flux into the North polar region from the tail of the magnetosphere. With a southward interplanetary magnetic field,  $B_s$ , magnetic flux enters the tail through the hatched region, whose area is  $2r_t R_E \times l_t R_E$ . Other symbols are defined in the text.

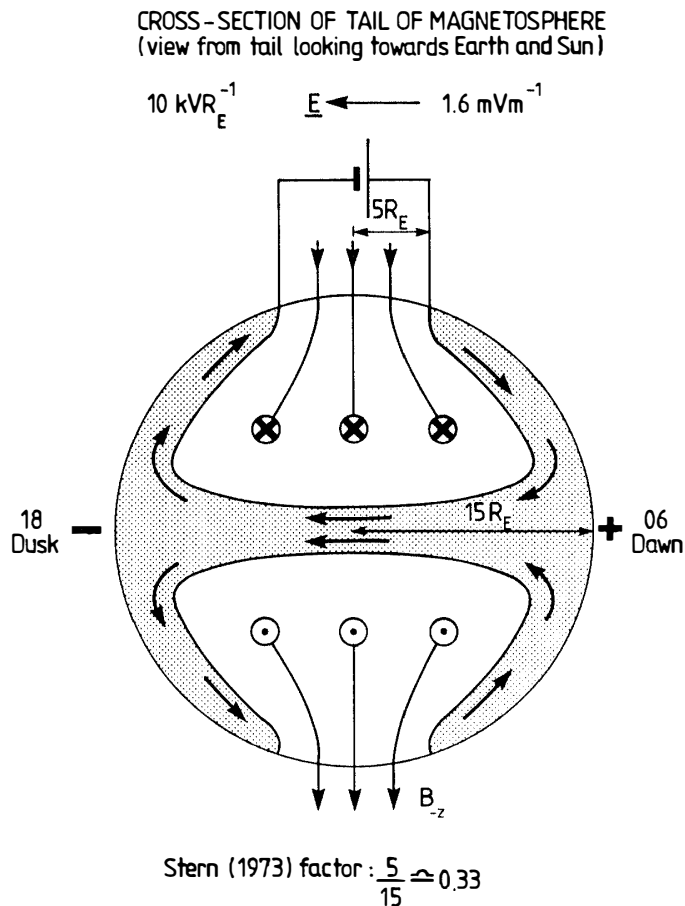


Fig. 7. Cross-section of the magnetospheric tail, showing the electromotive force associated with the solar wind-magnetosphere dynamo as a battery. Magnetic field lines entering the tail are shown, as are currents flowing in the tail magnetopause. The STERN (1973) factor is explained in the text.



by the position of the field line which is about to merge with another distended field line, from the southern hemisphere, in the neutral sheet region. The width of the hatched region of the tail, which is not so great as the width of the tail in the equatorial plane, is determined by the principle of the conservation of magnetic flux. When this theorem is applied, it is clear that the width of the tail through which magnetic flux enters from the interplanetary medium into the northern magnetotail is approximately one third of the total tail width. Thus the STERN (1973) factor, shown in Fig. 7, is one third, or  $5 R_E$  divided by  $15 R_E$ , the latter being the half width of the tail in the equatorial plane. As will be shown later, the dawn to dusk electric field across the region of flux entry into the magnetosphere, the total width of which is  $10 R_E$ , and associated with the MHD flow outside the magnetotail, is typically  $10 \text{ kV}/R_E$ , or  $1.6 \text{ mV/m}$ .

*Table 1. The fundamentals of magnetic flux conservation in the magnetosphere-ionosphere system. Most quantities are defined in the text or in Fig. 6;  $dA$  is an element of area,  $R_E$  is the Earth radius, and  $B_x = B_{-z}$  is the southward component of the interplanetary magnetic field.*

---

1.  $\Phi_{\text{pci}} = \iint B_{\text{pci}} \cdot dA = B_p \pi R_E^2 \sin^2 \theta_{\text{pci}}$
2.  $\Phi_{\text{ip}} = B_{-z} 2r_t l_t R_E^2$   
 $\therefore \sin^2 \theta_{\text{pci}} = \frac{2r_t l_t}{\pi B_p} B_{-z}$  neutral sheet in  $x, y$  plane
3.  $\Phi_{\text{ip}} = (B_y^2 + B_{-z}^2)^{1/2} 2r_t l_t R_E^2$  twisted neutral sheet  
 $\therefore \sin^2 \theta_{\text{pci}} = \frac{2r_t l_t}{\pi B_p} (B_y^2 + B_{-z}^2)^{1/2}$

---

Table 1 shows how the law of the conservation of magnetic flux from the southern polar cap through the magnetospheric tail and into the interplanetary medium relates important physical parameters, via the associated electric field in the interplanetary medium,  $E_{\text{ip}}$ . The amount of magnetic flux through the polar cap ionosphere,  $\Phi_{\text{pci}}$ , given in Table 1 as item 1, is related to the magnetic field at the magnetic pole,  $B_p$ , and the area of the polar cap, which depends upon  $\theta_{\text{pci}}$ , the co-latitude of the poleward edge of the auroral oval. Item 2 of Table 1 gives the magnetic flux entering the interplanetary medium,  $\Phi_{\text{ip}}$ , in terms of the southward component of the interplanetary magnetic field,  $B_{-z}$ , and the area of the shaded region in Fig. 6, which is taken to be rectangular. Equating these two magnetic flux values determines the size of the polar cap. Although, for simplicity, the magnetic field in interplanetary space is taken to have a purely southward component, the same theoretical concept can be applied when there is a dawn to dusk component of the interplanetary magnetic field also,  $B_y$ . In this case, the neutral sheet is twisted out of the equatorial plane, as sketched by COWLEY (1981). This is shown as item 3 in Table 1.

In Table 2, the average value of the electric potential difference directed from dawn to dusk across the polar cap ionosphere is given in item 1. Item 2 gives the electric field in the interplanetary medium and within the magnetotail; item 3 gives the potential difference in the solar wind, across the Stern window, taking the electric field to be uniform over a certain distance. Item 4 presents the essential result that,

by the conservation of magnetic flux, the potential difference across the polar cap ionosphere is equal to the potential difference across the outside of the magnetotail at the Stern window. The importance of this quantity has been succinctly stated by REIFF *et al.* (1981): “The electric potential drop across the Earth’s polar cap is a direct measure of the rate of plasma flow through the magnetospheric convection system. In future, continuous monitoring by true polar orbiting satellites and by probes in the upstream solar wind should enable us to develop a reliable scheme for predicting the polar cap potential drop from the parameters of the upstream solar wind.”

An alternative derivation of the results given in Table 2 can be achieved by apply-

*Table 2. The potential differences,  $V$ , and electric fields,  $E$ , associated with the application of Faraday’s law for the magnetic flux  $\Phi$  (from Table 1) and the full convection time  $T$ .*

---



---

Dawn-dusk potential difference $V$
Convection time, from “opening field line” at cusp to “closing it” at neutral sheet, $T = \frac{l_t R_E}{v_{1p}}$ in ionosphere
1. $V_{pc1} = E_{pc1} 2r_{pc1} = v_{pc1} B_p 2r_{pc1}$ $\therefore V_{pc1} = \frac{4r_{pc1}^2 B_p}{T} \simeq \frac{\Phi_{pc1}}{T}$
2. $E_{1p} = E_y = -(v_{-x} B_{-z} + v_z B_{-x})$ , $\frac{v_z}{v_{-x}} \simeq \tan \alpha < 1$ , tail flaring angle $\alpha$ $+v_z B_{-x}$ Away sector, northern hemisphere $-v_z B_{-x}$ Away sector, southern hemisphere $-v_z B_x$ Towards sector, northern hemisphere $+v_z B_x$ Towards sector, southern hemisphere
3. $V_{1p} = E_{1p} 2r_t R_E = v_{1p} B_{-z} 2r_t R_E$ in solar wind outside tail of magnetosphere $\therefore V_{1p} = \frac{l_t R_E}{T} B_{-z} 2r_t R_E = \frac{\Phi_{1p}}{T}$
4. If $\Phi_{pc1} = \Phi_{1p}$ , $V_{pc1} = V_{1p}$

---



---

*Table 3. Numerical values are given, self-consistently, for the algebraic symbols used in Tables 1 and 2. Using Fig. 8 as a calibration, the dimensions of the STERN (1973) window are deduced.*

---



---

1. $\Phi_{pc1} = 7.9 \times 10^9 \sin^2 \theta_{pc1}$ Wb Considering, under moderately disturbed conditions of geomagnetic activity, cusp at $78^\circ$ latitude, poleward edge of midnight aurora at $68^\circ$ , $\theta_{pc1} = 17^\circ$
2. With $\Phi_{pc1} = \Phi_{1p} = 6.8 \times 10^8$ Wb $r_t l_t R_E^2 = \frac{6.8 \times 10^8}{2B_{-z}}$ With $B_{-z} = 4$ nT, $r_t l_t = 2 \times 10^8$ , in units of $R_E^2$
3. Since $2 r_t R_E = \frac{V_{1p}}{v_{1p} B_{-z}}$ Using, as calibration, $\frac{V_{pc1}}{v_{1p} B_{-z}} = \frac{100 \text{ kV}}{1.6 \text{ mV m}^{-1}} = 6.25 \times 10^7$ m with $v_{1p} = 400 \text{ kms}^{-1}$ , $B_{-z} = 4$ nT (COWLEY, 1984; REIFF, 1984) With $V_{pc1} = V_{1p}$ , $r_t = 5 R_E$ $\therefore l_t = 400 R_E$ and $T = 106$ min, time constant for magnetospheric response to change of interplanetary magnetic field, such as sector boundary.

---



---

ing Faraday's law. This is that the  $\text{EMF} = -d\Phi/dt$ . For a steady process, the  $\text{EMF} = -\Phi/T$ .

Table 3 derives typical numerical values. Taking moderately disturbed conditions, with  $\theta_{\text{pcI}} = 17^\circ$ , a self-consistent set of values is obtained with a southward IMF of 4 nT, a solar wind speed of  $400 \text{ km s}^{-1}$  and a cross polar cap potential difference,  $V_{\text{pcI}}$ , of 100 kV. With the width of the Stern window discussed earlier, the full length of the geomagnetic tail, as defined earlier, is derived to be about  $400 R_E$ . It is the conservation of magnetic flux which determines the length of the tail once the width of the tail has been determined according to the potential difference across the magnetotail or polar cap.

Once the length of the tail is known the time constant for the total response of the magnetosphere to a change in solar wind conditions, for example a southward turning of the IMF, can be found. In this case, it is almost two hours. Of course, phenomena can be happening within the magnetosphere on a shorter timescale. For example, the time when a particular interplanetary magnetic flux tube is directly north of the neutral sheet merging region will (from Fig. 6) be approximately one third of this time, namely 35 min. A sudden increase in external pressure to the magnetosphere applied at this point at this time would propagate to the merging region within a minute or so, and this might trigger a substorm. Thus the time delay between a southward turning of the IMF and the onset of an auroral substorm would, on these

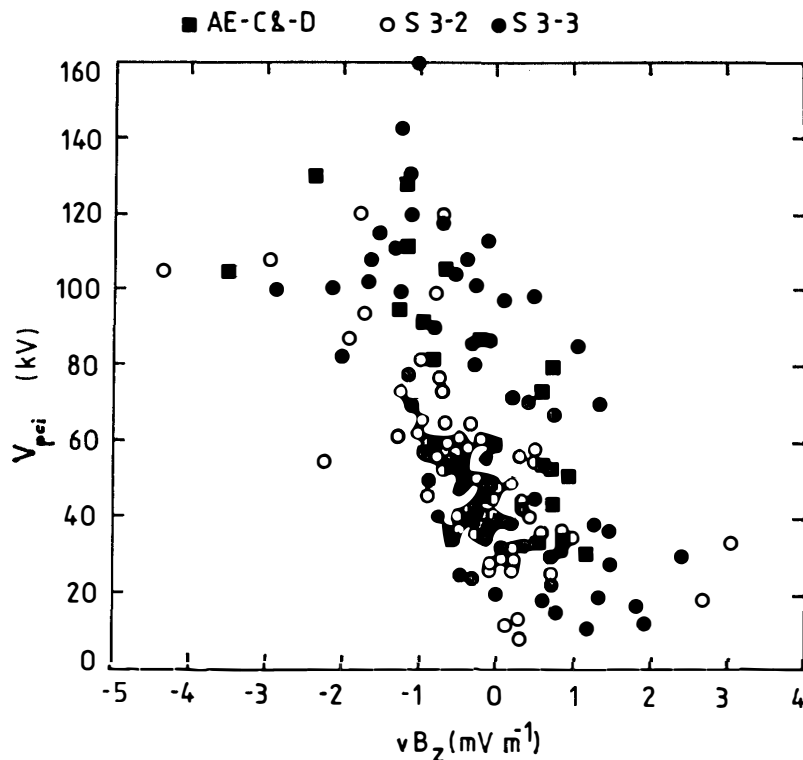


Fig. 8. Results, from COWLEY (1984), showing experimental data from four satellites on the potential difference across the polar cap ionosphere,  $V_{\text{pcI}}$ , as a function of the electric field  $E$  shown in Fig. 7; this is given as the product of the solar wind velocity,  $v$ , and the North-South component of the interplanetary magnetic field,  $E_z$ .

ideas, be expected to be 30 or 40 min. CLAUER *et al.* (1981) and BAKER *et al.* (1983) have analysed experimental data to show that these are typical observed values.

Figure 8, also reproduced from COWLEY (1984), shows that the value of 100 kV for  $V_{ip} = V_{pe1}$  at  $E_{ip} = -1.6 \text{ mV m}^{-1}$ , that is  $v_{ip} = 400 \text{ km s}^{-1}$  and  $B_{-z} = 4 \text{ nT}$ , is typical of conditions in the Earth's environment. An electric field strength of  $1.6 \text{ mV m}^{-1}$ , or  $10 \text{ kV } R_E^{-1}$  across the Stern window of the magnetotail, is equivalent to  $26 \text{ mV m}^{-1}$  in the polar cap ionosphere. Such a value is typical of the experimental values reported by HEPPNER and MAYNARD (1986). Further, TSURUTANI *et al.* (1984), presenting Fig. 9 which gives the percentage of occasions that the  $z$  component of the magnetic field in the plasma sheet has certain values, claimed that the distance to the merging region down the tail is scarcely ever less than  $80 R_E$ , and quite often near  $200 R_E$ . Thus a total length of the tail of  $400 R_E$  is eminently reasonable.

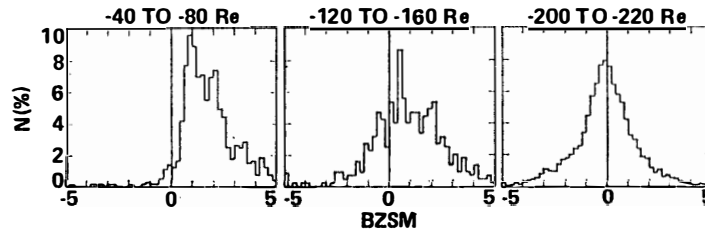


Fig. 9. ISEE-3 results from TSURUTANI *et al.* (1984), showing the proportion of occasions that the magnitude of the North-South component of the magnetic field in the plasma sheet within the tail of the magnetosphere has a certain value, at three different distance ranges down the tail.

Table 4. Further numerical values are given, which lead to the results depicted in Fig. 10.

- 
4.  $E_{ip} = \frac{100 \text{ kV}}{10 R_E} = 10 \text{ kV } R_E^{-1}$  or  $1.6 \text{ mV m}^{-1}$   
 $E_{pe1} = \frac{100 \text{ kV}}{34^\circ \times 111 \text{ km}^\circ^{-1}}$  or  $26 \text{ mV m}^{-1}$
  5. For change of  $B_{-z}$ , assuming  $r_t$ ,  $l_t$  and  $v_{ip}$  remaining constant  

$$\frac{d\Phi_{pe1}}{\Phi_{pe1}} \frac{dB_{-z}}{B_{-z}} = \frac{dV_{pe1}}{V_{pe1}} = \frac{dQ}{Q} = 0.035 \cot \theta_{pe1} d\theta_{pe1}$$
 $\approx 15\%$  per degree of latitude,  $\theta = 13^\circ$ , quiet conditions  
 $\approx 11\%$  per degree of latitude,  $\theta = 17^\circ$ , moderately disturbed conditions  
 $\approx 9\%$  per degree of latitude,  $\theta = 21^\circ$ , very disturbed conditions
- 

Another new result is shown in Table 4 (a continuation of Table 3), in terms of the change of polar cap dimensions corresponding to a change of interplanetary magnetic field strength,  $B_{-z}$ . As shown in item 5 of Table 4, all these quantities, generically  $Q$ , are proportionally related in an identical way with the dimensions of the polar cap. Thus, for moderately disturbed conditions when  $\theta_{pe1} = 17^\circ$ , the rate of change of all these quantities is 11% per degree of latitude of  $\theta_{pe1}$ . This result is depicted graphically in Fig. 10, a) showing the magnitude of the magnetic flux itself as a function of polar cap co-latitude; this curve is essentially parabolic. Differentiating this relationship, b) is obtained and this shows that the flux increment per degree of expanded polar cap is almost linearly dependent on the size of the polar cap itself.

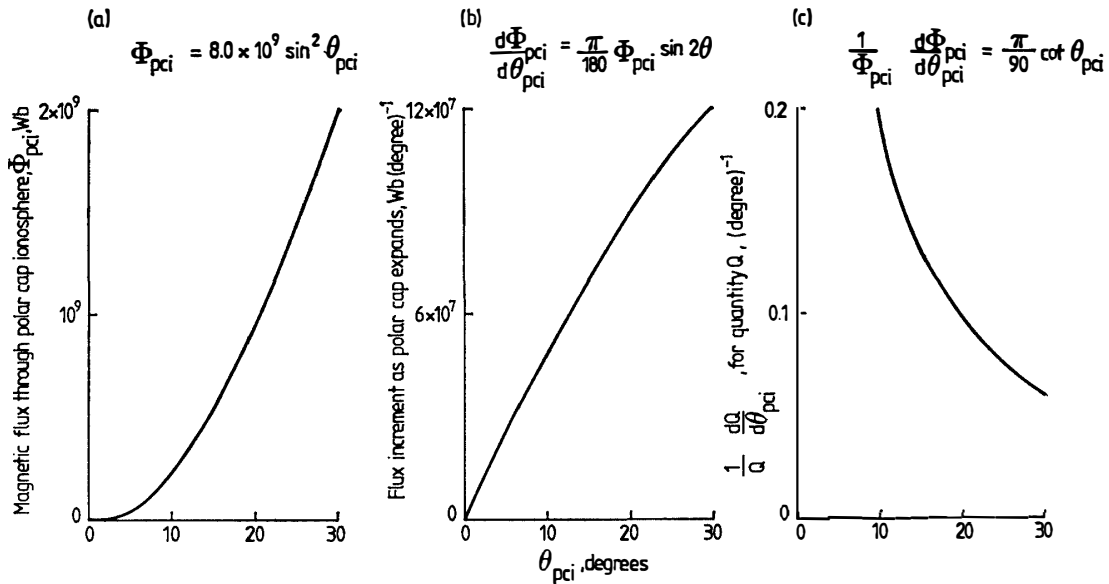


Fig. 10. (a) The magnetic flux through the polar cap, as a function of the half angle of the poleward boundary of the auroral oval,  $\theta_{pci}$ .  
 (b) The change of magnetic flux through the polar cap ionosphere,  $\Phi_{pci}$ , as the auroral oval expands.  
 (c) The fractional change in a quantity  $Q$ , that is proportional to the magnetic flux through the polar cap ionosphere,  $\Phi_{pci}$ , as the size of the auroral oval changes.

Finally, c) shows that the fractional change in these quantities is proportional to  $\cot \theta_{pci}$ . It would be extremely interesting to apply these relatively simple ideas to the observed changes in the dimensions of the polar cap as geomagnetic activity waxes and wanes, in response to changes of the IMF.

#### 4. Recent Observational Results and Prospects for Future Research

In order to investigate the physics of the geospace plasma, many different types of observational technique can give valuable information. For example, using satellites the velocity of the solar wind and the vector magnetic field in interplanetary space are crucial parameters. The size of the polar cap can be obtained from images of the auroral oval obtained from space, for example as taken from the Dynamics Explorer and Viking satellites, and measured in order to calculate the magnetic flux into the northern polar cap. Occasional DE images over Antarctica would, likewise, give the flux out of the southern polar cap. Polar orbiting satellites give information not only on the dawn to dusk cross polar cap potential difference,  $V_{pci}$ , but also, from their magnetic perturbations, field aligned currents,  $J_{||}$ . These currents close through the ionospheric plasma in the high latitude region and so it is important also to know the ionospheric conductivity, both Hall and Pedersen, and the flow velocities of the ionospheric plasma in the  $E$ - and  $F$ -regions.

Figure 11, from CARBARY and MENG (1986), shows eight hours of data on the interplanetary magnetic field north-south component, the latitude of the equatorward boundary of the cusp, as observed from a polar orbiting DMSP satellite, and the au-

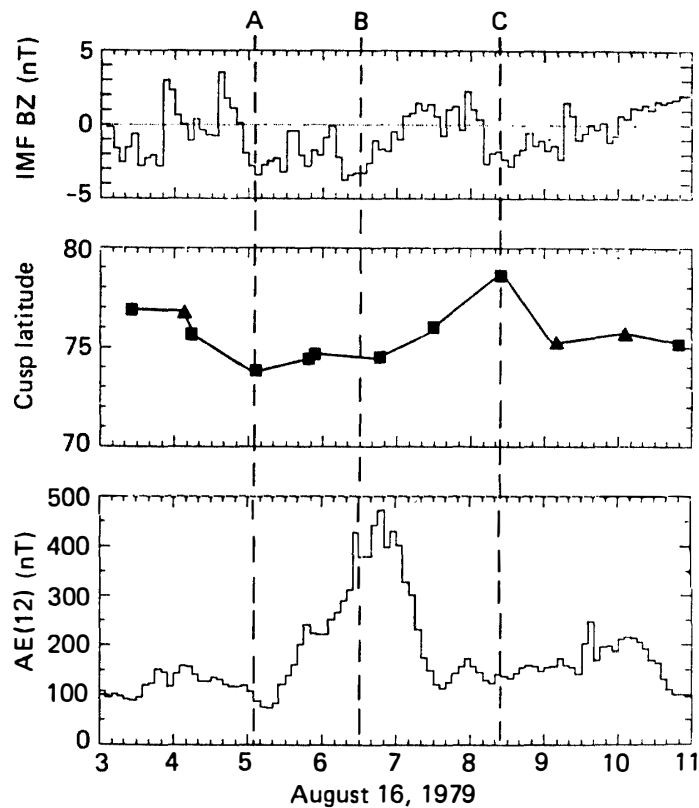


Fig. 11. From CARBARY and MENG (1986), this shows the North-South component of the interplanetary magnetic field, IMF BZ, for eight hours on 16 August 1979. Also shown are the location of the ionospheric signature of the magnetospheric cusp, and the auroral electrojet index.

roral electrojet ( $AE$ ) index at 5 min intervals. The data shown as squares are more reliable than those given as triangles. Generally speaking, it is believed that a southward turning of the interplanetary magnetic field causes the position of the cusp to move to lower latitudes. In this way, the magnetic flux linking interplanetary space to the polar cap increases, as considered in Fig. 10. Such an effect is noted near 04 UT, near 05 UT (A) and near 08 UT (C). However, the southward turning just after 06 UT (B) does not seem to enlarge the polar cap, although at this time the auroral electrojet currents become stronger. Whilst the theoretical concepts introduced earlier can explain some parts of this data set, they cannot explain all the changes, even for time scales of the order of 10 min or more.

IJIMA and POTEIRA (1976) demonstrated the location of both downward and upward field aligned currents in the polar regions. Since then, much has been written by a number of authors, including TROSHICHEV (1984), D'ANGELO (1980) and SAFLEKOS *et al.* (1982). The latter authors published Fig. 12, which shows the differences in spatial patterns of field aligned currents into the ionosphere or out of the ionosphere, crosses and circled dots respectively, for different values of the dawn to dusk ( $y$ ) component of the interplanetary magnetic field. The current systems are different in the northern and southern hemispheres, yet they exhibit some consistent relationships. Within two hours of 12 LT, near the ionospheric signature of the cusp, the current

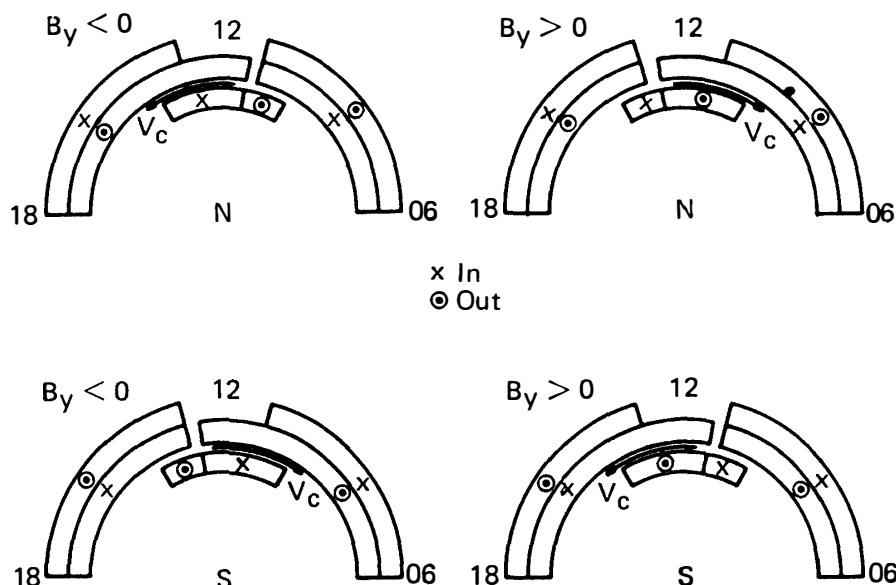


Fig. 12. Diagram, from SAFLEKOS *et al.* (1982), showing the direction of field aligned currents into ( $\times$ ) or out of ( $\odot$ ) the high latitude ionosphere, both North and South, as a function of local time through the day, for negative or positive values of the dawn-to-dusk component of the interplanetary magnetic field,  $B_y$ .

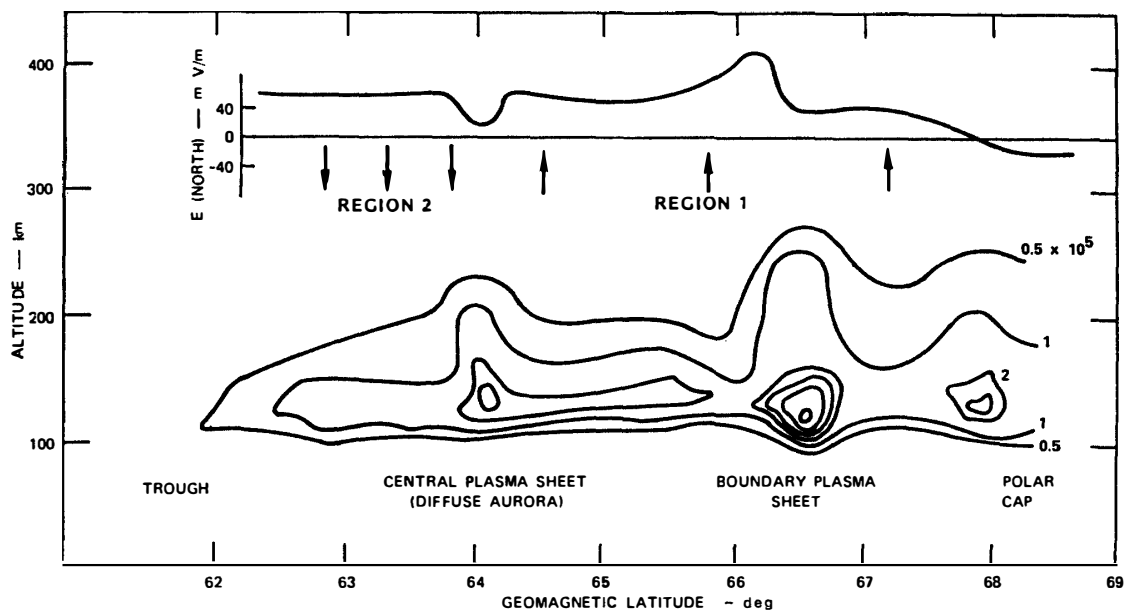


Fig. 13. Ionospheric electron density contours and, above, the location of region 1 and region 2 field aligned current systems, together with the northward component of the electric field in the evening ionosphere over a  $7^\circ$  latitude range. The associated features in the magnetosphere are named near the bottom of the figure (from VONDRAK, 1983).

systems are complex. Ionospheric electron density contours, taken from VONDRAK (1983), are related to the different regions of field aligned currents as shown at the top of Fig. 13. Also shown are the ionospheric features which are believed to be linked along geomagnetic flux tubes to significant regions of the magnetosphere. Shown

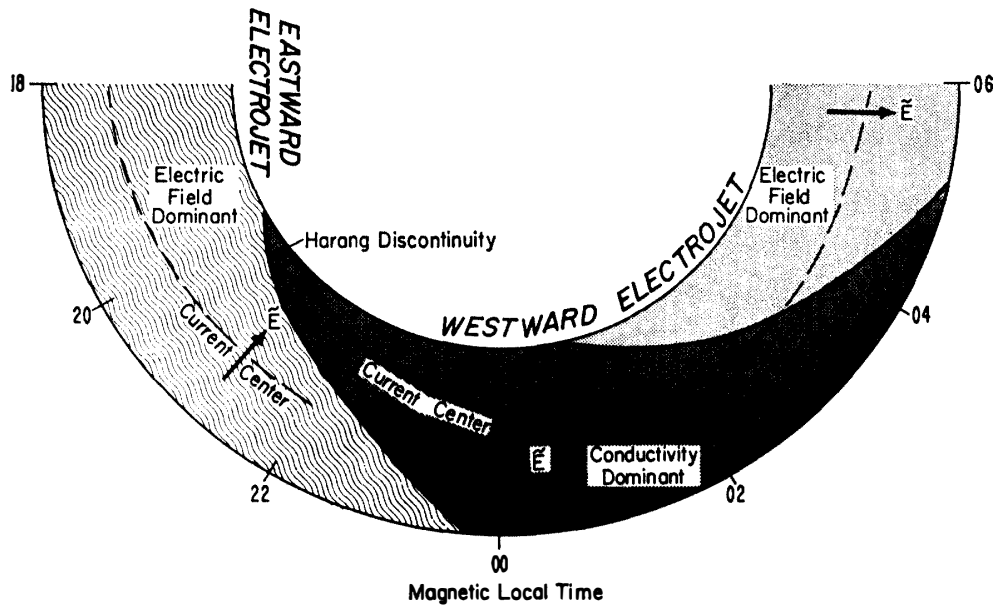


Fig. 14. Diagram showing regions in the auroral ionosphere through the night where either the electric field determines the magnitude of the ionospheric electric currents (nearer dusk or dawn) or the ionospheric conductivity limits the current (near magnetic midnight).

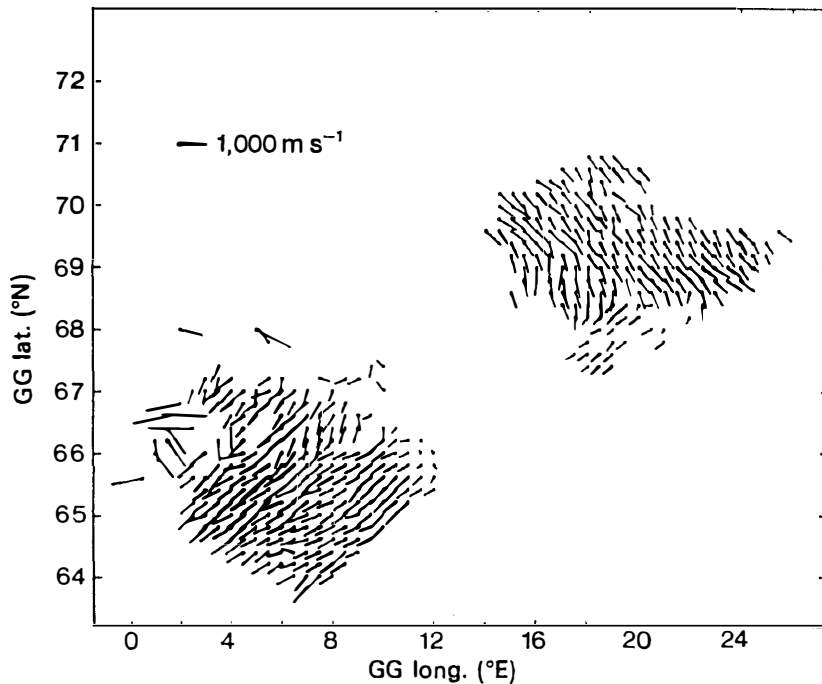


Fig. 15. Radar results map the E-region plasma drift velocities, from BURRAGE et al. (1985); for details, see text.

here in Fig. 13 for evening conditions are plasma concentration values, the plasma being at least partly created by the precipitation of energetic charged particles which are responsible for the auroral luminosity. KAMIDE and VICKREY (1983) and KAMIDE (1984) discuss Fig. 14 on the different parts of the auroral oval, at different times through



the night, where the ionospheric electric currents are determined predominantly by the electric field (before midnight) or by the ionospheric conductivity, mainly after midnight. Regions in the ionosphere where the electric field is poleward, before midnight, and equatorward after midnight, are separated by the Harang discontinuity.

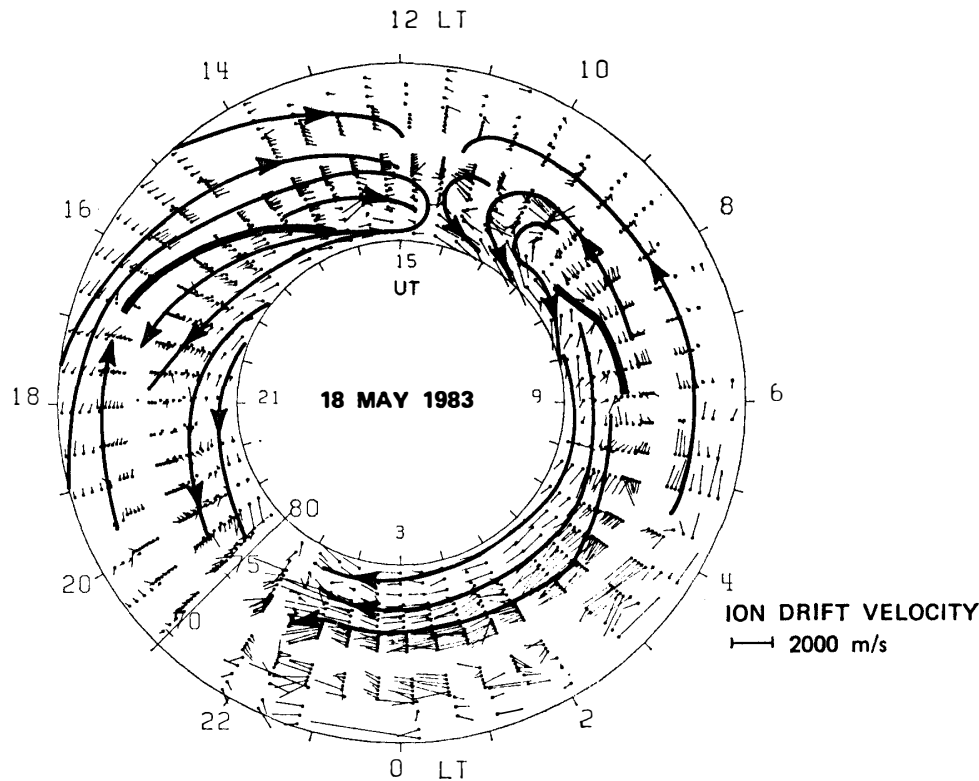


Fig. 16. Sondre Stromfjord incoherent scatter radar results on *F*-region plasma motions, from KELLY (1985); for details, see text.

From BURRAGE *et al.* (1985), Fig. 15 shows SABRE (lower left) and STARE (right) radar data on *E*-region plasma drift velocities. In the vicinity of the Harang discontinuity, these data obtained at 1911 UT on 6 September 1982 demonstrate the flow reversal near  $68.5^{\circ}\text{N}$ ,  $20^{\circ}\text{E}$  geographic. *F*-region plasma drift patterns are conveniently recorded by incoherent scatter radars. Twenty-four hours of data recorded on 18 May 1983 at Sondre Stromfjord, Greenland, are depicted in Fig. 16. The twin cell convection pattern is very clearly evident. The cusp which occurs at 1130 LT corresponds to a rotation reversal, and there is a shear reversal in the centre of each twin cell convection pattern, as shown by the bold line. Another incoherent scatter radar located in the auroral zone is EISCAT, Northern Scandinavia. Figure 17 shows EISCAT data that have been interpreted to give field aligned currents within the radar's field of view, for 16 June 1982. The observed plasma convection paths are interpreted to be driven by electric fields to which they are related by the MHD equations. The electric fields are interpreted to give a pattern which, combined with the Hall and Pedersen conductivities in the *E*-region obtained from plasma density measurements, gives the horizontal component of the ionospheric electric currents. From the divergence of these currents, the magnitude of the field aligned currents is obtained. The

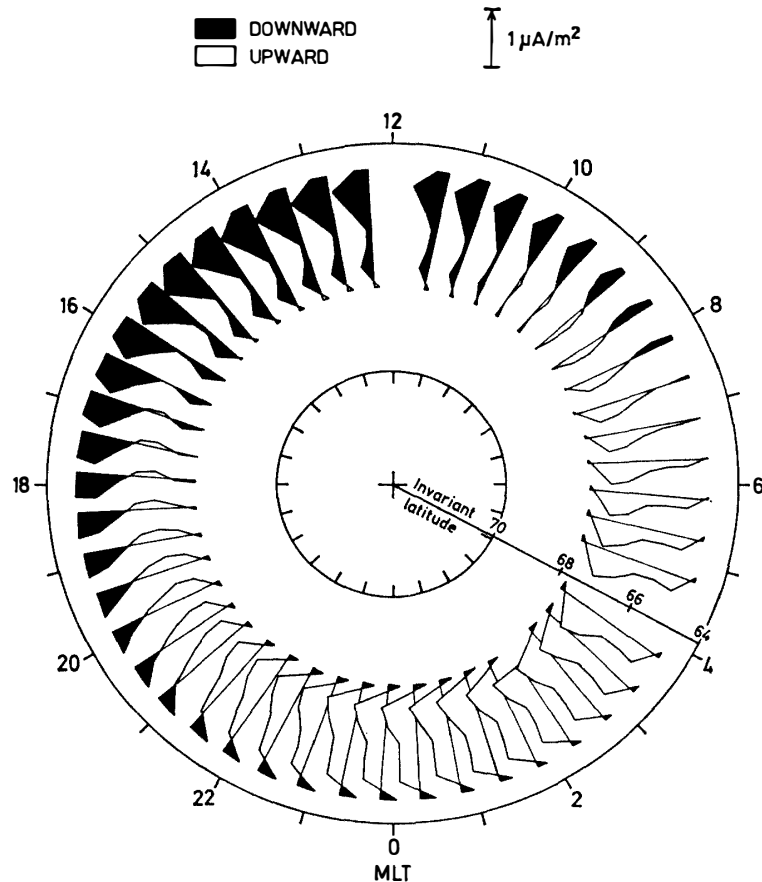


Fig. 17. EISCAT incoherent scatter radar results on derived field aligned currents, from EISCAT Annual Report (EUROPEAN INCOHERENT SCATTER SCIENTIFIC ASSOCIATION, 1984); for details, see text.

upward (region 1) current system is clearly seen, as is the downward (region 2) current system.

GREENWALD *et al.* (1985) have presented data giving *F*-region convection patterns observed by a backscatter radar operating at Goose Bay in Labrador and viewing the region over Sondre Stromfjord. The Doppler shift in the signal backscattered by *F*-region irregularities is interpreted to give plasma convection velocities. A data set recorded during 24 h can be used to map out the polar cap convection paths. For the future, funding has recently be granted for a joint American/British radar to be installed at Halley, Antarctica. The viewing area of this radar will be poleward from Halley, towards and beyond the South Pole. The viewing area of this radar is geomagnetically conjugate to the area viewed by the Labrador radar. In a few years, exciting results should be obtained on the geomagnetic conjugacy, or otherwise, of plasma convection patterns in the polar cap. It will be extremely interesting to see how these conjugate ionospheres behave, as functions of season and time, not to mention interplanetary magnetic field directions.

The field of endeavour discussed here is ripe for joint international projects. Planning of these projects can be well done by bodies such as SCOSTEP and SCAR; since they are international, the spirit of the Antarctic Treaty is made manifest by

such work. Comparisons between ground-based, balloon, rocket and satellite experiments will continue to be valuable for the remainder of the century. Planned for this period are the International Solar Terrestrial Physics (ISTP program) and the Solar Terrestrial Energy Program (STEP). Such programmes will concentrate upon the macro-scale physics of geospace, which can often be interpreted within the framework of magnetohydrodynamics. However, it should always be remembered that some phenomena, such as micro-scale wave-particle interactions, require more detailed electrodynamic treatment. The interaction between whistler mode waves and energetic electrons in the magnetosphere is an example of a wave-particle interaction process whereby magnetospheric physics influences ionospheric phenomena on a much shorter time scale and smaller space scale, but that topic is another subject worthy of a separate paper.

### References

- AKASOFU, S.-I. (1980): What is a magnetospheric substorm? Dynamics of the Magnetosphere, ed. by S.-I. AKASOFU. Dordrecht, D. Reidel, 447–460.
- ALFVÉN, H. (1981): Cosmic Plasma. Dordrecht, D. Reidel, 164p.
- ATKINSON, G. (1979): The expansive phase of the magnetospheric substorm. Dynamics of the Magnetosphere, ed. by S.-I. AKASOFU. Dordrecht, D. Reidel, 461–481.
- ATKINSON, G. (1984): The role of currents in plasma redistribution. Magnetospheric Currents. Washington, D.C., Am. Geophys. Union, 325–330 (Geophys. Monogr., **28**).
- BAKER, D. N., ZWICKL, R. D., BAME, S. J., HONES, E. W., Jr., TSURUTANI, B. T., SMITH, E. J. and AKASOFU, S.-I. (1983): An ISEE 3 high time resolution study of interplanetary parameter correlations with magnetospheric activity. J. Geophys. Res., **88**, 6230–6242.
- BURRAGE, M. D., WALDOCK, J. A., JONES, T. B. and NIELSEN, E. (1985): Joint STARE and SABRE radar auroral observations of the high-latitude ionospheric convection pattern. Nature, **316**, 133–135.
- CARBARY, J. F. and MENG, C.-I. (1986): Relations between the interplanetary magnetic field  $B_z$ ,  $AE$  index, and cusp latitude. J. Geophys. Res., **91**, 1549–1556.
- CLAUER, C. R., MCPHERSON, R. L., SEARLS, C. and KIVELSON, M. G. (1981): Solar wind control of auroral zone geomagnetic activity. Geophys. Res. Lett., **8**, 915–918.
- COWLEY, S. W. H. (1980): Plasma populations in a simple open model. Space Sci. Rev., **26**, 217–275.
- COWLEY, S. W. H. (1981): Magnetospheric asymmetries associated with the Y-component of the IMF. Planet. Space Sci., **29**, 79–96.
- COWLEY, S. W. H. (1984): Solar wind control of magnetospheric convection. Proc. Conf. Achievements of the IMS, Graz, Austria. ESA SP-217, 483–494.
- D'ANGELO, N. (1980): Field aligned currents and large scale magnetospheric electric fields. Ann. Geophys., **36**, 31–40.
- DUNGEY, J. W. (1965): The length of the magnetospheric tail (letters). J. Geophys. Res., **70**, 1753.
- EUROPEAN INCOHERENT SCATTER SCIENTIFIC ASSOCIATION (1984): EISCAT Annual Report. Sweden, 14p.
- GREENWALD, R. A., BAKER, K. B., HUTCHINS, R. A. and HANUISE, C. (1985): An HF phase-array radar for studying small-scale structure in the high-latitude ionosphere. Radio Sci., **20**, 63–79.
- HEPPNER, J. P. and MAYNARD, N. C. (1986): Empirical high latitude electric field models, preprint. Maryland, NASA.
- IJIMA, T. and POTEMRA, T. A. (1976): Field-aligned currents in the dayside cusp observed by Triad. J. Geophys. Res., **81**, 5971–5979.
- KAMIDE, Y. (1984): IMS advances in studies of field-aligned currents and their related electrodynamic. Proc. Conf. Achievements of the IMS, Graz, Austria. ESA SP-217, 243–256.

- KAMIDE, Y. and VICKREY, J. F. (1983): Relative contribution of ionospheric conductivity and electric field to the auroral electrojets. *J. Geophys. Res.*, **88**, 7989–7996.
- KELLY, J. D. (1985): Incoherent scatter radar observations of the cusp. *The Polar Cusp*, ed. by J. A. HOLTET and A. EGELAND. Dordrecht, D. Reidel, 337–348.
- MCILWAIN, C. E. (1961): Coordinates for mapping the distribution of magnetically trapped particles. *J. Geophys. Res.*, **66**, 3681–3691.
- MCPHERRON, R. L. (1979): Magnetospheric substorms. *Rev. Geophys. Space Phys.*, **17**, 657–681.
- POTEMRA, T. A. and ZANETTI, L. J. (1985): Characteristics of large-scale Birkeland currents in the cusp and polar regions. *The Polar Cusp*, ed. by J. A. HOLTET and A. EGELAND. Dordrecht, D. Reidel, 203–222.
- REIFF, P. H., SPIRO, R. W. and HILL, T. W. (1981): Dependence of polar cap potential drop on interplanetary parameters. *J. Geophys. Res.*, **86**, 7639–7648.
- SAFLEKOS, N. A., SHEEHAN, R. E. and CAROVILLANO, R. L. (1982): Global nature of field-aligned currents and their relation to auroral phenomena. *Rev. Geophys. Space Phys.*, **20**, 709–734.
- SONNERUP, B. U. Ö. (1985): Solar wind interaction with planetary magnetic fields. *Proc. ESA Workshop on Future Missions in Solar, Heliospheric and Space Plasma Physics, Garmisch-Partenkirchen, Germany*. ESA SP-235, 53–64.
- STERN, D. P. (1973): A study of the electric field in an open magnetospheric model. *J. Geophys. Res.*, **78**, 7292–7305.
- TROSHICHEV, O. A. (1984): Solar wind control of electric fields and currents in the magnetosphere and ionosphere. *Proc. Conf. Achievements of the IMS, Graz, Austria*. ESA SP-217, 407–416.
- TSURUTANI, B. T., SLAVIN, J. A., SMITH, E. J., OKIDA, R. and JONES, D. E. (1984): Magnetic structure of the distant geotail from  $-60$  to  $-220 R_e$ ; ISEE-3. *Geophys. Res. Lett.*, **11**, 1–4.
- VONDRAK, R. (1983): Incoherent scatter radar measurements of electric field and plasma in the auroral ionosphere. *High-Latitude Space Plasma Physics*, ed. by B. HULTQVIST and T. HAGFORS. New York, Plenum Press, 73–93.

( Received December 6, 1986 )